

# **Rapidity scan with multistage hydrodynamic and statistical thermal models**

Lipei Du, Han Gao, Sangyong Jeon, Charles Gale

**arxiv: 2302.13852**

# Framework

(3+1)-dimensional multistage model: MUSIC+IS3D+UrQMD

MUSIC: a hydrodynamics model with parametric initial conditions

PRC.82.014903  
PRC.93.044906  
PRC.98.034916

NEOS-B: EoS combined LQCD at high T and HRG at low T

PRC 100, 024907

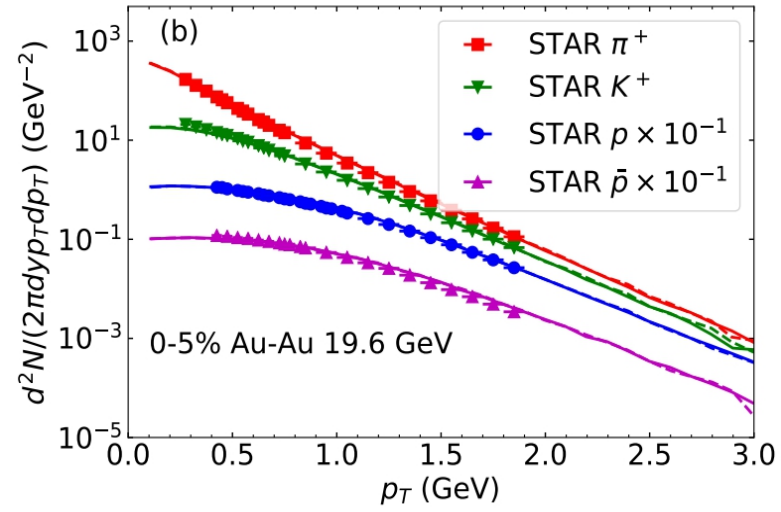
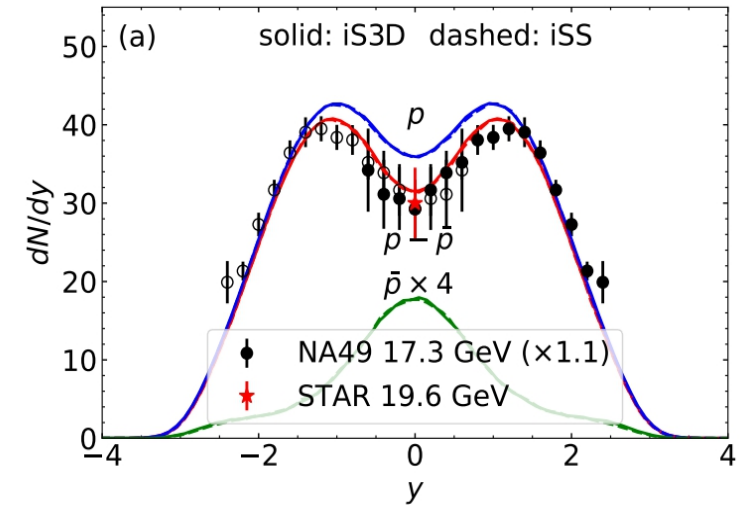
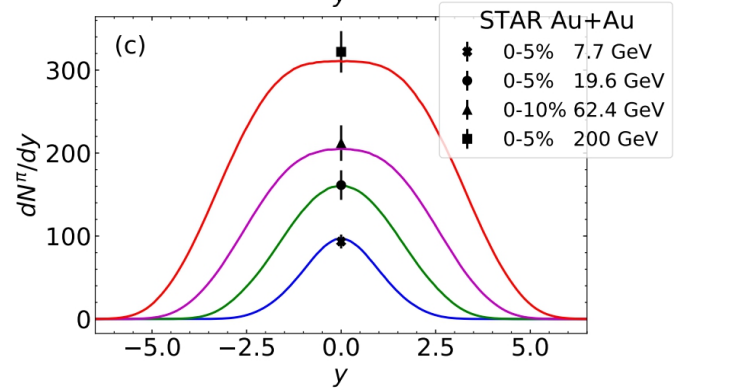
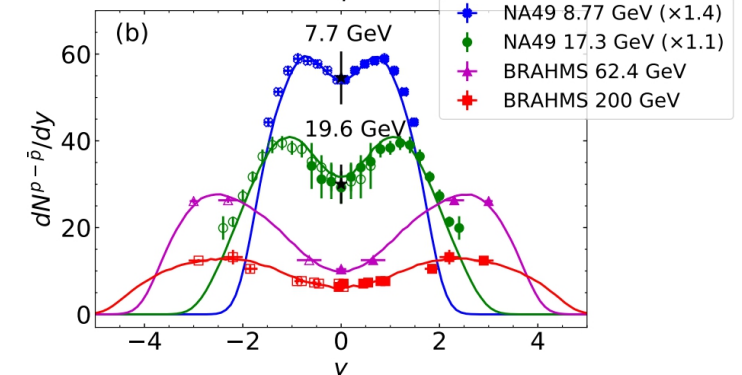
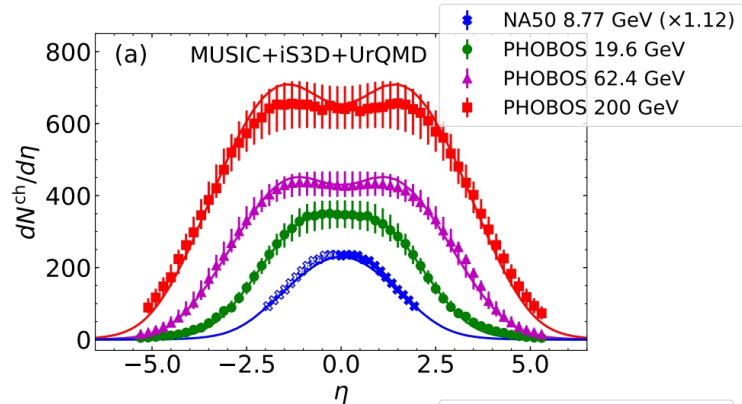
IS3D: sample hadrons on the freeze-out surface

arxiv: 1912.08271

UrQMD: a transport model simulating hadronic afterburner

J. Phys. G 25, 1859-1896

# Calibration



# Statistical Thermal Model

Cooper-Frye prescription: 
$$E_p \frac{dN_h}{d^3p} = \frac{g_h}{(2\pi)^3} \int_{\Sigma} p \cdot d^3\sigma(x) f_h(x, p)$$

Phys. Rev. D 10, 186 (1974)

discretized

$$E_p \frac{dN_h^i}{d^3p} = \frac{g_h}{(2\pi)^3} [p \cdot d^3\sigma(x_i)] f_h(x_i, p)$$

$$E_p \frac{dN_h}{d^3p} = \frac{dN_h}{dy_h m_T dm_T d\phi_h} = \frac{g_h V}{(2\pi)^3} E_p f_h$$

proton distribution

$$\left. \frac{dN_p}{dy} \right|_{y_s=0} = \frac{g_p VT^3}{(2\pi)^2} \left( \frac{2}{\cosh^2 y} + \frac{m_p}{T} \frac{2}{\cosh y} + \frac{m_p^2}{T^2} \right) \times \exp\left(\frac{\mu - m_p \cosh y}{T}\right),$$

pi+&K+ distribution

$$\left. \frac{dN_i}{dy} \right|_{y_s=0} = \frac{g_i VT^3}{(2\pi)^2} \sum_{n=1}^{\infty} \left(\frac{1}{n}\right)^3 \left( \frac{2}{\cosh^2 y} + \frac{nm_i}{T} \frac{2}{\cosh y} + \frac{n^2 m_i^2}{T^2} \right) \exp\left(-\frac{nm_i \cosh y}{T}\right), \quad (10)$$

**discrete source model:** assume all the particles at rapidity  $y$  are emitted from a thermal source at the same rapidity  $y_s$ , i.e.,  $y_s = y$ .

net-proton yield 
$$N_{p-\bar{p}} = \frac{g_p VT}{2\pi^2} m_p^2 K_2(\beta m_p) 2 \sinh \beta \mu$$

pi/K yield 
$$N_i = \frac{g_i VT}{2\pi^2} m_i^2 \sum_{n=1}^{\infty} \frac{1}{n} e^{n\beta \mu} K_2(n\beta m_i)$$

**single source model:** integrate out  $y$  from the rapidity dependent yields to obtain the full phase space yields (or  $4\pi$ -yields)

**continuous source model:** the measured yields at a specific rapidity  $y$  can have contributions from the sources with thermal smearing in a finite window of  $y_s$

# Results

the space-time distribution of thermodynamic quantities on the freeze-out surface

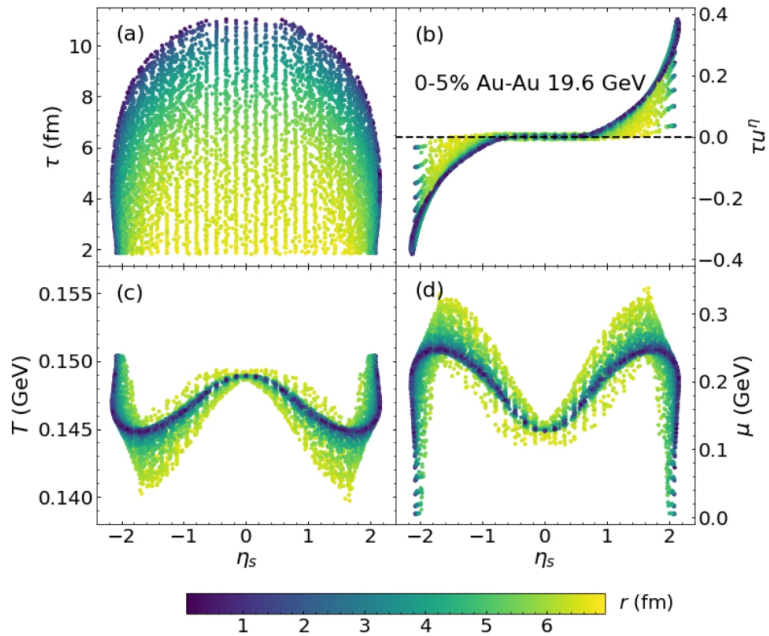


FIG. 3. Distributions in space-time rapidity  $\eta_s$  of freeze-out cells at  $e_{fo} = 0.26 \text{ GeV}/\text{fm}^3$  for 0-5% Au+Au collisions at  $\sqrt{s_{NN}} = 19.6 \text{ GeV}$ : (a) longitudinal proper time  $\tau$ , (b) longitudinal flow  $\tau u^n$ , (c) temperature  $T$  and (d) baryon chemical potential  $\mu$ . The colors represent the radial distance  $r = \sqrt{x^2 + y^2}$  of a fluid cell from the transverse center of the fireball. Cells with dark green are near the fireball center, and light yellow ones are towards the edge.

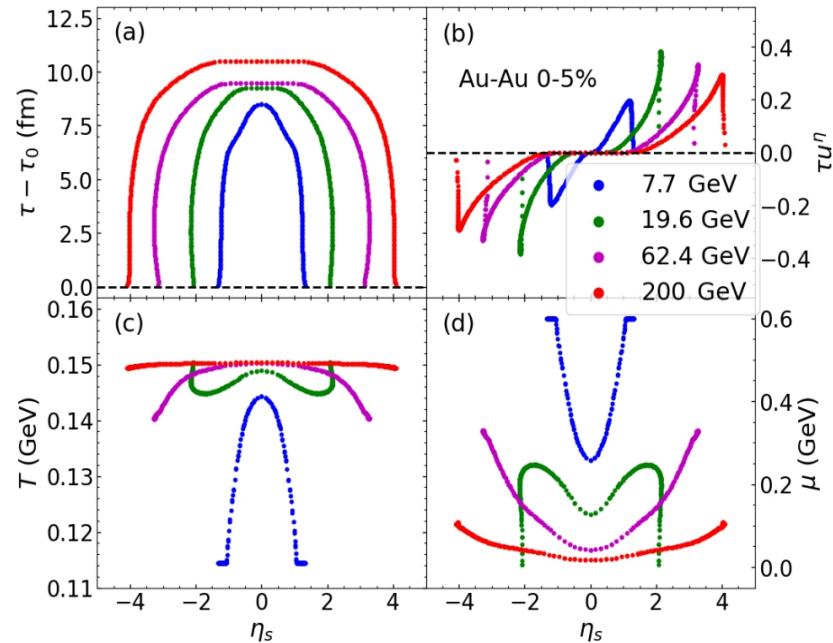


FIG. 4. Similar to Fig. 3 but for 0-5% Au+Au collisions at four beam energies. Here we focus on the fluid cells near the fireball's transverse center, i.e., in the case of 19.6 GeV, the dark green ones shown in Fig. 3. In panel (a), the initialization time  $\tau_0$  has been subtracted from the proper time at different beam energies.

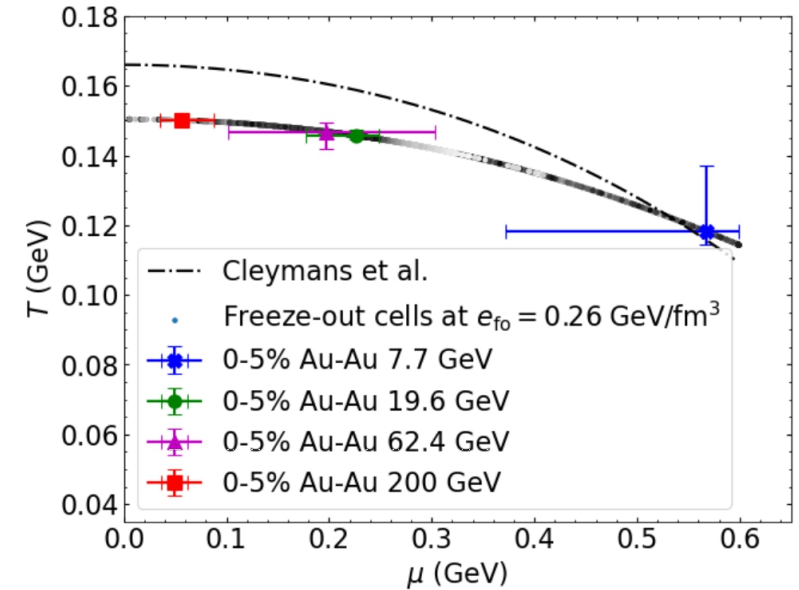


FIG. 5. Distributions of  $(T, \mu)$  in the phase diagram for the fluid cells on the freeze-out surfaces from 0-5% Au+Au collisions at the four beam energies. The grayish scatter points represent the freeze-out fluid cells at  $e_{fo} = 0.26 \text{ GeV}/\text{fm}^3$ . The four markers with error bars illustrate the medians and 25% and 75% percentiles of  $(T, \mu)$  distributions for the freeze-out cells at the four beam energies. As a comparison, the black dot-dashed line represents the chemical freeze-out line extracted using statistical thermal models from Ref. [24].

## Freeze-out profiles from thermal models

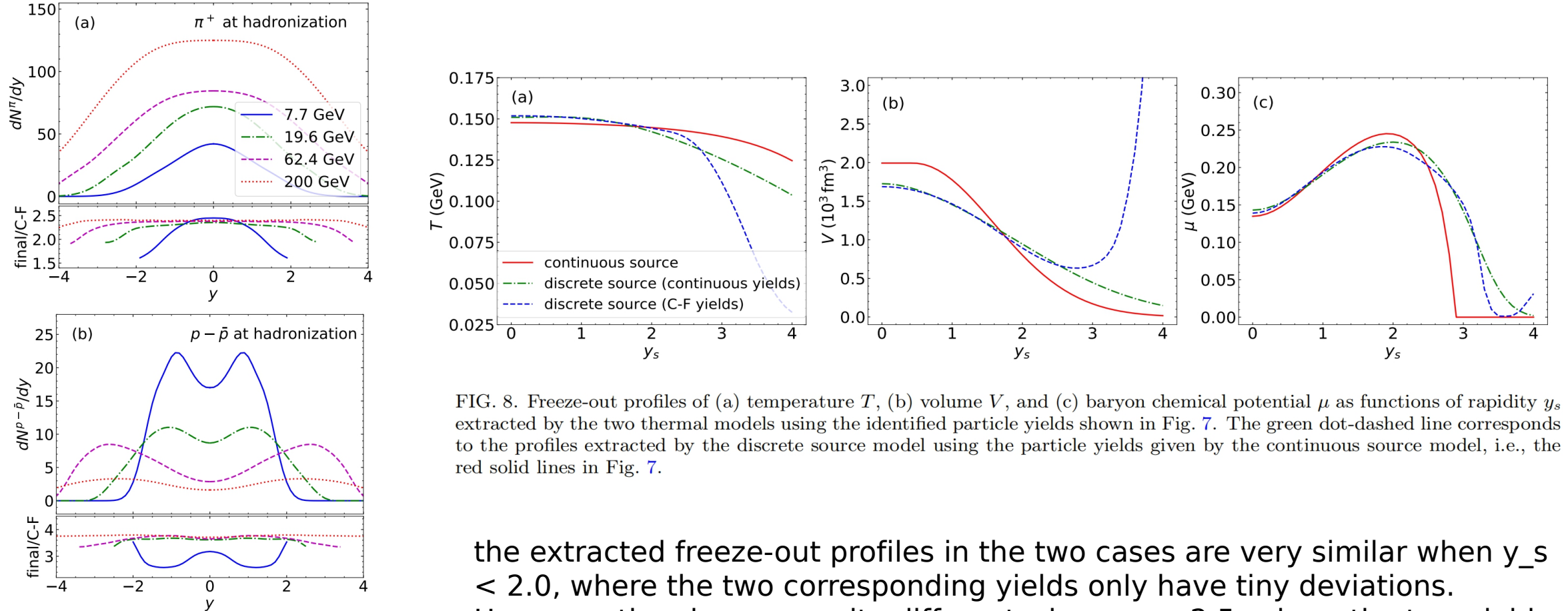


FIG. 8. Freeze-out profiles of (a) temperature  $T$ , (b) volume  $V$ , and (c) baryon chemical potential  $\mu$  as functions of rapidity  $y_s$  extracted by the two thermal models using the identified particle yields shown in Fig. 7. The green dot-dashed line corresponds to the profiles extracted by the discrete source model using the particle yields given by the continuous source model, i.e., the red solid lines in Fig. 7.

the extracted freeze-out profiles in the two cases are very similar when  $y_s < 2.0$ , where the two corresponding yields only have tiny deviations. However, they become quite different when  $y_s > 2.5$ , where the two yields are slightly different.

the results given by the three models are more consistent when the beam energy is higher, and thus the fireball is more homogeneous.

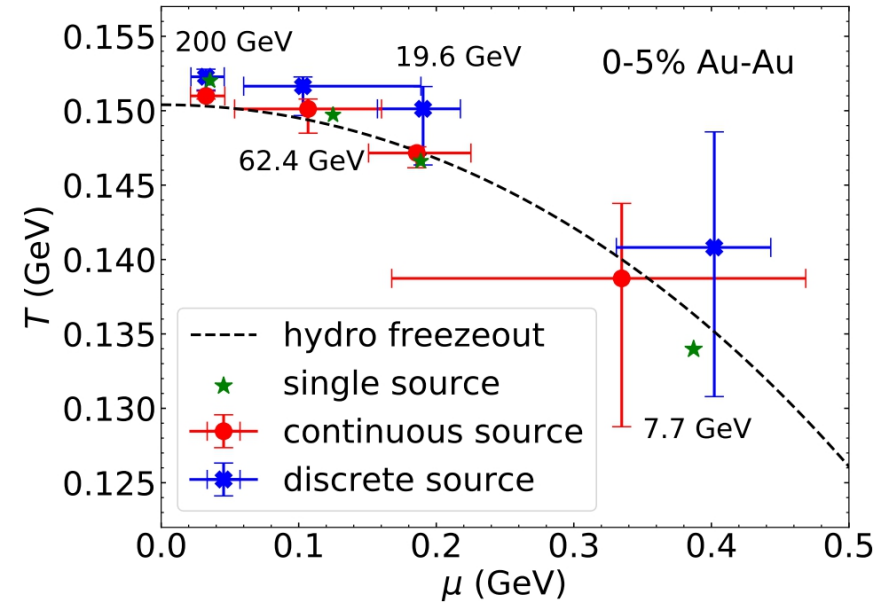


FIG. 9. Distributions of  $(T, \mu)$  in the phase diagram extracted by different scenarios of the thermal models for 0-5% Au+Au collisions at the four beam energies. The black dashed line shows a function  $T(\mu)$  fitted to the hydrodynamic freeze-out line in Fig. 5. The markers with error bars represent the median, and 25% and 75% percentiles of  $(T, \mu)$  distributions for the two scenarios of the thermal model. The red circles represent the continuous source model, and the blue x-markers the discrete source model. The green stars also show the results obtained from the single source model for comparison.



**Thanks**